Electron-Transfer Kinetics of Copper(II/I) Macrocyclic Tetrathiaether Complexes. Influence of Ring Size upon Gated Behavior

Gregory H. Leggett,[1a] Brian C. Dunn,[1a] Ana M. Q. Vande Linde,[1a] L. A. Ochrymowycz,[1b] and D. B. Rorabacher*,[1a]

Departments of Chemistry, Wayne State University, Detroit, Michigan 48202, and University of Wisconsin—Eau Claire, Eau Claire, Wisconsin 54701

Received June 9, 1993®

The values of the electron self-exchange rate constants, $k_{11(ex)}$, for the copper(II/I) complexes formed with the cyclic tetrathiaethers [13]aneS$_4$ and [15]aneS$_4$ have been determined using ^{1}H-NMR line-broadening measurements in D_2O at several different temperatures to yield the following results for 25 °C, corrected to μ = 0.1 M (NO_3^-): for $Cu^{II/I}$([13]aneS$_4$), $k_{11(ex)} = 3.2 \times 10^5$ M^{-1} s^{-1}, $\Delta H^{\ddagger} = 10 \pm 1$ kJ mol^{-1}, $\Delta S^{\ddagger} = -106 \pm 7$ J K^{-1} mol^{-1}; for $Cu^{II/I}$([15]aneS$_4$), $k_{11(ex)} = 1.2 \times 10^4$ M^{-1} s^{-1}, $\Delta H^{\ddagger} = 21 \pm 1$ kJ mol^{-1}, $\Delta S^{\ddagger} = -97 \pm 7$ J K^{-1} mol^{-1}. The cross-reaction rate constants have also been determined in aqueous solution by means of stopped-flow methods for these complexes reacting with a series of selected oxidants and reductants: $Co^{II}(Me_4[14]tetraeneN_4)(H_2O)_2$, $Ru^{II}(NH_3)_4bpy$, $Ru^{II}(NH_3)_5py$, $Ru^{II}(NH_3)_6$, $Co^{III}(Me_4[14]tetraeneN_4)(H_2O)_2$, $Ru^{III}(NH_3)_4bpy$, $Ni^{III}([14]aneN_4)(H_2O)_2$, $Ru^{III}(NH_3)_2(bpy)_2$, and $Fe^{III}(4,7\text{-}Me_2phen)_3$. The self-exchange rate constants calculated by applying the Marcus relationship to the rate constants for reactions involving $Cu^{II}L$ reduction ($k_{11(Red)}$) are within experimental error of each other and agree with the $k_{11(ex)}$ values determined by NMR. However, as in earlier studies, the self-exchange rate constant values calculated from $Cu^{I}L$ oxidation reactions ($k_{11(Ox)}$) are generally smaller, except for very slow cross reactions. This pattern of behavior is in agreement with our previously proposed dual-pathway square scheme in which conformational change and the electron-transfer step occur in a sequential, rather than a concerted, manner. For the $Cu^{II/I}$([13]aneS$_4$) system, a lower limit of $k_{RP} \geq 200$ s^{-1} is estimated for the rate constant representing the conformational change from the ground state Cu(I) species to the metastable intermediate which precedes the electron transfer step via the preferred pathway. For the $Cu^{II/I}$([15]aneS$_4$) system, a rough limit of $k_{RP} \leq 5$ s^{-1} is suggested by the data. Moreover, for this latter system, the secondary pathway was found to be more competitive than is the case for either the $Cu^{II/I}$([13]aneS$_4$) system or the previously studied $Cu^{II/I}$([14]aneS$_4$) system, so that gated behavior is anticipated to occur only within a very narrow set of conditions.

Introduction

Studies on $Cu^{II/I}L$ systems (L = coordinated ligand) have often yielded inconsistent results for the kinetics of $Cu^{II}L$ reduction as compared to $Cu^{I}L$ oxidation.[2] In earlier work,[3] we surveyed the electron-transfer kinetics for a variety of Cu(II/I)–polythiaether complexes reacting with both a selected oxidant (A_{Ox}) and a reductant (A_{Red}):

$$Cu^{II}L + A_{Red} \underset{k_{21}}{\overset{k_{12}}{\rightleftharpoons}} Cu^{I}L + A_{Ox} \qquad (1)$$

The resultant k_{12} and k_{21} values were then inserted into the Marcus relationship[4] to generate the apparent self-exchange rate constants, k_{11} (as defined by reaction 2). On the basis of these

$$*Cu^{II}L + Cu^{I}L \overset{k_{11}}{\rightleftharpoons} *Cu^{I}L + Cu^{II}L \qquad (2)$$

calculations, we noted that the values obtained from $Cu^{II}L$ reduction ($k_{11(Red)}$) were generally 30- to 10^7-fold larger than the corresponding values calculated from $Cu^{I}L$ oxidation ($k_{11(Ox)}$).

Scheme I

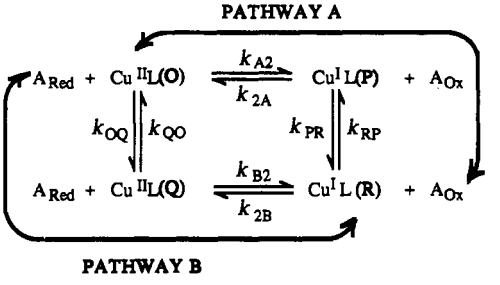

To explain these discrepancies, we proposed that the $Cu^{II/I}L$ systems react by a dual-pathway square scheme mechanism in which conformational changes and the electron-transfer step occur in a sequential rather than a concerted manner. As depicted in Scheme I, this mechanism entails two metastable intermediate species, Q and P, which are presumed to differ conformationally (or configurationally) from the corresponding ground state species, designated as O and R.

Both Hoffman and Ratner[5] and Brunschwig and Sutin[6] have described the theoretical behavior to be expected for square

• Abstract published in *Advance ACS Abstracts*, November 15, 1993.

(1) (a) Wayne State University. (b) University of Wisconsin—Eau Claire.

(2) (a) Augustin, M. A.; Yandell, J. K. *J. Chem. Soc., Chem. Commun.* **1978**, 370–372. (b) Augustin, M. A.; Yandell, J. K.; Addison, A. W.; Karlin, K. D. *Inorg. Chim. Acta* **1981**, *55*, L35–L37. (c) Yoneda, G. S.; Blackmer, G. L.; Holwerda, R. A. *Inorg. Chem.* **1977**, *16*, 3376–3378. (d) Lee, C.-W.; Anson, F. C. *J. Phys. Chem.* **1983**, *87*, 3360–3362.

(3) Martin, M. J.; Endicott, J. F.; Ochrymowycz, L. A.; Rorabacher, D. B. *Inorg. Chem.* **1987**, *26*, 3012–3022.

(4) (a) Marcus, R. A. *J. Chem. Phys.* **1956**, *24*, 966–978. (b) Marcus, R. A. *Discuss. Faraday Soc.* **1960**, *29*, 21–31. (c) Marcus, R. A. *J. Chem. Phys.* **1965**, *43*, 679–701. (d) Marcus, R. A.; Sutin, N. *Biochim. Biophys. Acta* **1985**, *811*, 265–322.

(5) (a) Hoffman, B. M.; Ratner, M. A. *J. Am. Chem. Soc.* **1987**, *109*, 6237–6243. Cf., correction: *Ibid.* **1988**, *110*, 8267. (b) Hoffman, B. M.; Ratner, M. A.; Wallin, S. A. In *Electron Transfer in Biology and the Solid State*; Advances in Chemistry Series Vol. 226; Johnson, M. K., King, R. B., Kurtz, D. M., Jr., Kutal, C., Norton, M. L., Scott, R. A., Eds.; American Chemical Society: Washington, DC, 1990; pp 125–146.

(6) (a) Brunschwig, B. S.; Sutin, N. *J. Am. Chem. Soc.* **1989**, *111*, 7454–7465. (b) Sutin, N.; Brunschwig, B. S. In *Electron Transfer in Biology and the Solid State*; Advances in Chemistry Series Vol. 226; Johnson, M. K., King, R. B., Kurtz, D. M., Jr., Kutal, C., Norton, M. L., Scott, R. A., Eds.; American Chemical Society: Washington, DC, 1990; pp 65–88.

0020-1669/93/1332-5911$04.00/0

schemes of this type. They have specifically noted that, under appropriate conditions, the reaction may become rate limited by either of the conformational changes O ⇌ Q or P ⇌ R (but not both) depending upon the relative stabilities of the two intermediate species (P and Q). For thermodynamically favorable reactions, the theory predicts that such conformationally-controlled behavior will be manifested in only one direction.[6a] The onset of conformational control, a first-order process, has been termed "gated"[5] or "directional"[6] electron-transfer.

For $Cu^{II/I}([14]aneS_4)$, we have used low-temperature[7a] and rapid-scan[7b] cyclic voltammetry to demonstrate not only the

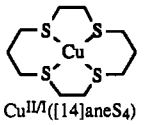

$Cu^{II/I}([14]aneS_4)$

existence of both species P and Q, but also the fact that P is more stable than Q for this specific system. This implies that, under slow-exchange conditions, pathway A is preferred over pathway B and, as conditions are changed to accelerate the electron-transfer step, the conformational change R→P should eventually become rate-limiting. The results of an extensive study on the cross-reaction electron-transfer kinetics of $Cu^{II/I}([14]aneS_4)$, involving a total of eight counter reagents, made it possible to demonstrate the onset of conformationally-limited electron-transfer kinetics for the *oxidation* of the Cu(I) complex as predicted.[8] Ultimately, a switch to pathway B occurred for the most rapid oxidation reactions studied. On the basis of both the electrochemical and cross-reaction studies, all of the stepwise rate constants in Scheme I have now been estimated for the $Cu^{II/I}([14]aneS_4)$ system.[7b,8]

To date, the presence of a dual-pathway square scheme mechanism has not been thoroughly demonstrated for any other Cu(II/I) system. Thus, it remains to be established whether Scheme I applies to other (perhaps all) Cu(II/I) systems as we have proposed. Moreover, for all systems for which Scheme I does apply, it has now become clear that the evaluation of the electron-transfer behavior requires thorough kinetic measurements on both the oxidation and reduction kinetics with several counter reagents exhibiting differing potentials and self-exchange rate constant values.

In the current work, we have attempted to demonstrate the existence of a dual-pathway mechanism for two closely related systems, $Cu^{II/I}([13]aneS_4)$ and $Cu^{II/I}([15]aneS_4)$, by measuring

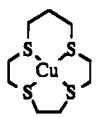

$Cu^{II/I}([13]aneS_4)$

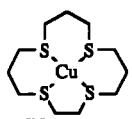

$Cu^{II/I}([15]aneS_4)$

their electron-transfer kinetics with a variety of counter reductants and oxidants. We have also used ^{1}H-NMR line-broadening measurements on each system to obtain direct values for the self-exchange rate constants. In this investigation, our major goals were to determine whether the patterns in the various calculated k_{11} values were in conformance with Scheme I and to determine the effect of variable ring size upon the overall kinetic behavior.

The two ligand systems selected for this study were chosen as representative of the two major types of $Cu^{II}L$ geometries which have been determined crystallographically for complexes with

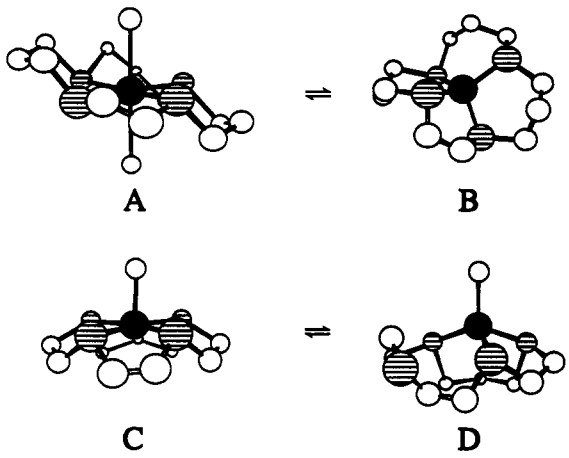

Figure 1. Proposed ground-state geometries for (A) $Cu^{II}([15]aneS_4)$, (B) $Cu^{I}([15]aneS_4)$, (C) $Cu^{II}([13]aneS_4)$, and (D) $Cu^{I}([13]aneS_4)$ based on known crystal structures for these or related species (see text). Hydrogen atoms have been omitted for clarity. The solid and shaded spheres represent the copper atom and the sulfur donor atoms, respectively. The ligands on the vertical axes in species A, C, and D are presumed to be water molecules in aqueous solution.

cyclic tetrathiaethers:[9] (i) $Cu^{II}([15]aneS_4)$ is similar in structure to $Cu^{II}([14]aneS_4)$, existing as a six-coordinate complex with the four sulfur donor atoms occupying the sites in the plane and two anions or solvent molecules occupying the two axial sites (Figure 1A). (ii) By contrast, the $Cu^{II}([13]aneS_4)$ complex exists as a five-coordinate square pyramidal complex with the four sulfur donor atoms occupying the sites in the basal plane and a solvent molecule or anion occupying the apical site (Figure 1C). To date, we have been unable to obtain satisfactory crystal structures for the Cu(I) species for these same two systems. However, these systems should also provide examples of the two coordination types which have been demonstrated to exist for $Cu^{I}L$ species with cyclic tetrathiaethers: (i) $Cu^{I}([15]aneS_4)$ is predicted to exist as a somewhat flattened tetrahedron in which all four thiaether sulfur donor atoms remain coordinated to the Cu(II) ion (Figure 1B)—as has been observed crystallographically for $Cu^{I}([14]aneNS_3)$.[10] (ii) $Cu^{I}([13]aneS_4)$ is expected to adopt an irregular tetrahedral arrangement in which one Cu–S bond is ruptured such that the inner-coordination sphere consists of three thiaether sulfur donor atoms and a solvent molecule (Figure 1D).[11]

On the basis of the foregoing considerations, it was anticipated that at least one of the systems in the current study should involve a significantly different conformational change than that which exists for the $[14]aneS_4$ system. This presumption suggested that a comparison of the kinetic behavior for $Cu^{II/I}([13]aneS_4)$ and $Cu^{II/I}([15]aneS_4)$ with that reported for $Cu^{II/I}([14]aneS_4)$ would provide further insight into the manifestations of structural constraints upon the overall electron-transfer behavior.

For the purpose of these studies, the reductants selected as counter reagents were $Co^{II}(Me_4[14]tetraeneN_4)(H_2O)_2$, $Ru^{II}(NH_3)_4bpy$, $Ru^{II}(NH_3)_5py$, and $Ru^{II}(NH_3)_6$, while the oxidants included $Co^{III}(Me_4[14]tetraeneN_4)(H_2O)_2$, $Ru^{III}(NH_3)_4$-bpy, $Ni^{III}([14]aneN_4)(H_2O)_2$, $Ru^{III}(NH_3)_2(bpy)_2$, and $Fe^{III}(4,7\text{-}Me_2phen)_3$ (where $Me_4[14]tetraeneN_4$ represents 2,3,9,10-

(7) (a) Bernardo, M. M.; Robandt, P. V.; Schroeder, R. R.; Rorabacher, D. B. *J. Am. Chem. Soc.* **1989**, *111*, 1224–1231. (b) Robandt, P. V.; Schroeder, R. R.; Rorabacher, D. B. *Inorg. Chem.* **1993**, *32*, 3957–3963.

(8) Meagher, N. E.; Juntunen, K. L.; Salhi, C. A.; Ochrymowycz, L. A.; Rorabacher, D. B. *J. Am. Chem. Soc.* **1992**, *114*, 10411–10420.

(9) Pett, V. B.; Diaddario, L. L., Jr.; Dockal, E. R.; Corfield, P. W. R.; Ceccarelli, C.; Glick, M. D.; Ochrymowycz, L. A.; Rorabacher, D. B. *Inorg. Chem.* **1983**, *22*, 3661–3670.

(10) Bernardo, M. M.; Heeg, M. J.; Schroeder, R. R.; Ochrymowycz, L. A.; Rorabacher, D. B. *Inorg. Chem.* **1992**, *31*, 191–198.

(11) Molecular models indicate that the 13-membered ring is too small to permit tetrahedral coordination with all four ligand donor atoms. The proposed geometry involving three coordinated sulfur donor atoms and a solvent molecule is inferred from a polymeric crystal structure obtained for $Cu^{I}([14]aneS_4)$: (a) Dockal, E. R.; Diaddario, L. L.; Glick, M. D.; Rorabacher, D. B. *J. Am. Chem. Soc.* **1977**, *99*, 4530–4532. (b) Diaddario, L. L., Jr.; Dockal, E. R.; Glick, M. D.; Ochrymowycz, L. A.; Rorabacher, D. B. *Inorg. Chem.* **1985**, *24*, 356–363.

tetramethyl-1,4,8,11-tetraazacyclotetradeca-1,3,8,10-tetraene, py and bpy represent pyridine and 2,2′-bipyridine, respectively, [14]-aneN$_4$ represents 1,4,8,11-tetraazacyclotetradecane, and 4,7-Me$_2$-phen represents 4,7-dimethyl-1,10-phenanthroline).

Experimental Section

Reagents. The preparation and purification of all reagents, including $Cu(ClO_4)_2{\cdot}6H_2O$ and $NaClO_4$,[12] [13]aneS$_4$ and [15]aneS$_4$,[13] and all counter reagents,[3,8] have been previously described. Solutions of the Cu^{I}L species were prepared by reduction with copper shot carried out under a nitrogen atmosphere. Distilled–deionized water of conductivity grade was used for the preparation of all solutions used for cross-reaction kinetic measurements. Ionic strength was controlled by the addition of $HClO_4$ or $NaClO_4$ except for the NMR studies for which nitrate salts were used. Argon or nitrogen was bubbled through all solutions prior to each kinetic run in order to remove dissolved oxygen. All ruthenium solutions were protected from light.

Instrumentation. Absorbance measurements were obtained using a Cary Model 17 dual-beam recording spectrophotometer equipped with a thermostated cell compartment. Kinetic measurements were made using a thermostated Durrum D-110 stopped-flow spectrophotometer equipped with "airtight" syringes. Absorbance data were recorded in digital form and then treated using either of the methods previously described.[3,8]

All ^{1}H-NMR spectra for line-broadening experiments and T_1 relaxation measurements were recorded on a Nicolet NT 300-MHz spectrometer equipped with a variable temperature unit and a Nicolet NMC 1280 data system. For the free ligands, the ^{1}H-NMR spectra were recorded in $CDCl_3$ to circumvent the low solubility of these ligands in aqueous media. The spectra of the corresponding Cu^{I}L species were recorded in D_2O using a one-pulse sequence. Selective decoupling experiments were used to assign the peaks. The specific methods used for obtaining the NMR relaxation data were identical to those described previously.[14] Other NMR measurements, such as homonuclear decoupling and ^{13}C spectral determinations, were recorded on a GE QE 300-MHz spectrometer.

Results

NMR Spectra. The ^{1}H spectrum for uncomplexed [13]aneS$_4$ is illustrated in Figure 2A. The peak integrations are in the ratio 6:2:1 leading unequivocally to the assignments shown. For the Cu^I([13]aneS$_4$) complex, the spectrum shows three sets of broad peaks. The peaks at 2.11 and 2.25 ppm are assigned to the protons on C-1 according to the possible structures of the complex as illustrated in Figure 2B. It is presumed that only three of the four sulfur donor atoms are coordinated to the copper ion since the ring would appear to be too small to accommodate tetrahedral coordination.[11] The broadness of the peaks indicates that the bond-breaking and bond-forming processes between Cu(I) and the sulfur donor atoms fall into the slow-exchange regime. At higher temperatures, in fact, the C-1 peaks coalesce into a single peak.

The observed ^{1}H spectrum of the uncomplexed [15]aneS$_4$ ligand is shown in Figure 3A. The spectrum consists of a singlet at 2.79 ppm which is the resonance signal of the C-3 protons on the ethylene bridge, a double-triplet at 2.67 ppm assigned to the protons on the α-carbons (C-2) of the trimethylene bridges, and a quintet at 1.93 ppm assigned to the protons on the central carbons (C-1) of the trimethylene bridges. Upon coordination to Cu(I), the environment of the C-1 and C-2 protons splits as illustrated in Figure 3B. The two quintets at 2.14 and 2.06 ppm exhibit a 1:2 ratio and correspond to the protons bonded to carbons labeled C-1 and C-1′, respectively. The triplets on the C-2 protons are split into three groups designated as C-2, C-2′ and C-2″. The well-defined ^{1}H spectrum for Cu^I([15]aneS$_4$) does suggest that

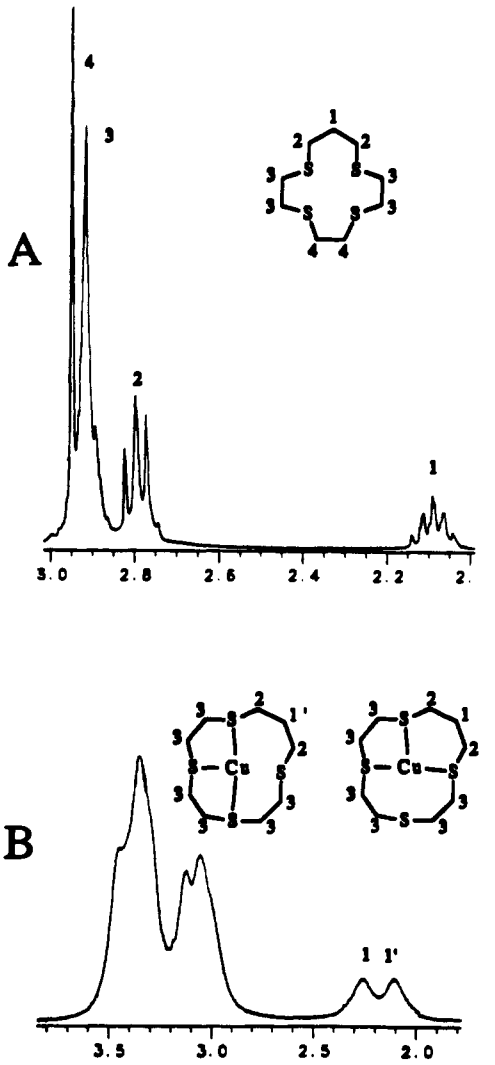

Figure 2. ^{1}H-NMR spectrum for (A) the [13]aneS$_4$ ligand in $CDCl_3$ and (B) the Cu^I([13]aneS$_4$) complex in D_2O, showing the assignments of the various peaks.

all four sulfur donor atoms are coordinated to the Cu(I) atom forming a symmetrical tetrahedral geometry. The average value of $^3J_{H-H}$ in the complex is 5.49 Hz.

Self-Exchange Kinetic Studies. The determination of the self-exchange electron-transfer reaction kinetics for Cu$^{II/I}$([13]aneS$_4$) and Cu$^{II/I}$([15]aneS$_4$) were carried out in the same manner as previously described for Cu$^{II/I}$([15]aneS$_5$),[14] Cu$^{II/I}$([15]aneNS$_4$),[15] and Cu$^{II/I}$([14]aneS$_4$)[8] by measuring the relaxation times for interconversion between diamagnetic (Cu^{I}L) and paramagnetic (Cu^{II}L) species, based on the expression derived by McConnell and Berger[16] as rearranged to the following form:[14]

$$(W_{DP} - W_D)Q\pi = k_{11(ex)}[Cu^{II}L] \qquad (3)$$

In eq 3, W_D represents the line width when only the diamagnetic species (Cu^{I}L) is present, W_{DP} is the corresponding line width after the addition of the paramagnetic species (Cu^{II}L), and the term Q is inserted to correct for the extent of outer-sphere complex formation at the specific ionic strength used to a common ionic strength value of 0.10 M.[14] A large excess of aquacopper(II) ion was added to all solutions to force the complexation of added

(12) Diaddario, L. L.; Zimmer, L. L.; Jones, T. E.; Sokol, L. S. W. L.; Cruz, R. B.; Yee, E. L.; Ochrymowycz, L. A.; Rorabacher, D. B. *J. Am. Chem. Soc.* **1979**, *101*, 3511–3520.
(13) Ochrymowycz, L. A.; Mak, C. P.; Michna, J. D. *J. Org. Chem.* **1974**, *39*, 2079–2084.
(14) Vande Linde, A. M. Q.; Juntunen, K. L.; Mols, O.; Ksebati, M. B.; Ochrymowycz, L. A.; Rorabacher, D. B. *Inorg. Chem.* **1991**, *30*, 5037–5042.
(15) Vande Linde, A. M. Q.; Westerby, B. C.; Ochrymowycz, L. A.; Rorabacher, D. B. *Inorg. Chem.* **1993**, *32*, 251–257.
(16) McConnell, H. M.; Berger, S. B. *J. Chem. Phys.* **1957**, *27*, 230–234. The approach described in this paper is an extension of the method developed by Gutowsky *et al.*: Gutowsky, H. S.; McCall, D. W.; Slichter, C. P. *Ibid.* **1953**, *21*, 279–292.

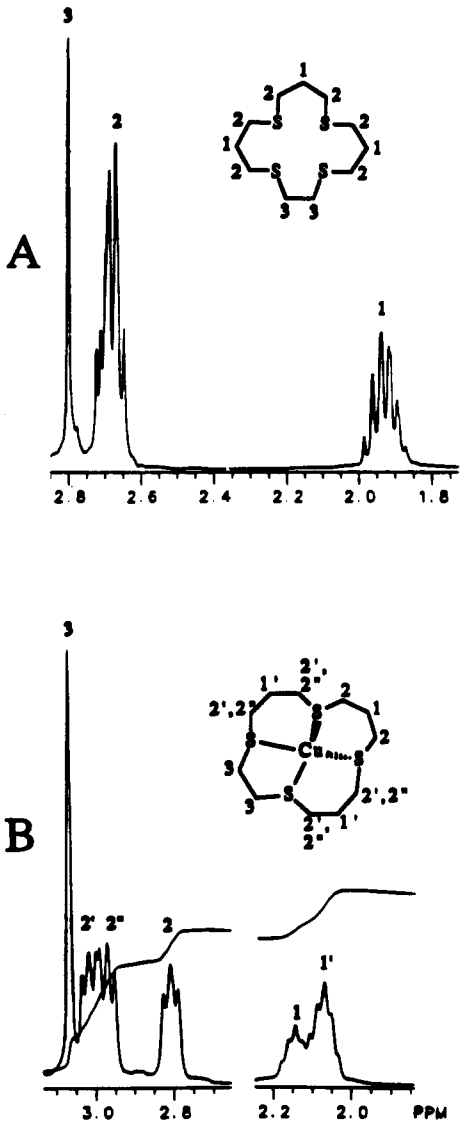

Figure 3. ^{1}H-NMR spectrum for (A) the [15]aneS$_4$ ligand in $CDCl_3$ and (B) the Cu^I([15]aneS$_4$) complex in D_2O, showing the assignments of the various peaks.

Cu^{II}L toward completion. The resultant paramagnetic line broadening induced by the Cu_{aq}^{2+} ion was shown to be essentially constant for all measurements.

For the Cu$^{II/I}$([13]aneS$_4$) system, the relative insolubility of the Cu(I) complex and the lack of a sharply defined peak were limiting factors in the data resolution. The best data were obtained by resolving the doublet at 2.1 ppm (Figure 2B). However, over the temperature range 5–35 °C, the spectrum was poorly resolved and it was not possible to obtain accurate deconvolution of the overlapping peaks in this region. Above 35 °C, however, these peaks coalesced as noted above. Thus, only line-width data obtained in the temperature range 45–65 °C were used for data analysis. A single series of measurements was made at pD 4.6 using a Cu^{I}L concentration of 7.9×10^{-4} M, a constant excess concentration of Cu$^{II}_{aq}$ at 0.10 M, and a Cu^{II}L concentration which was varied over the range 0–3.3×10^{-4} M. Plots of the resulting data for each temperature are shown in Figure 4. The resolved $k_{11(ex)}$ values are listed in Table I.

For Cu$^{II/I}$([15]aneS$_4$), the line-width measurements were made by deconvoluting the peaks in the region of 3.04 ppm (Figure 3B). Two separate series of solutions were prepared, both carried out at pD 4.6 under similar conditions but with a 10-fold change in the amount of aquacopper(II) ion present: (a) The first series contained 9.1×10^{-3} M Cu^{I}L and 0.010 M excess Cu$^{II}_{aq}$ with the Cu^{II}L concentration varied up to 2.4×10^{-5} M. (b) The second series contained 5.6×10^{-3} M Cu^{I}L and 0.10 M excess Cu$^{II}_{aq}$ with the Cu^{II}L concentration ranging up to 5.1×10^{-5} M. (See Supplementary Material for the line-width data.) Under these conditions, the amount of line broadening observed was relatively small. Plots for the data from one of the series of measurements are illustrated in Figure 5. As listed in Table I, the two series yielded very similar resolved $k_{11(ex)}$ values and activation parameters (as evaluated from the Eyring equation).

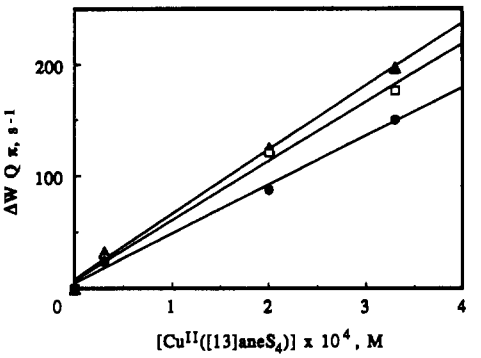

Figure 4. Plot of eq 3 for the NMR line-width data for Cu^I([13]aneS$_4$) as a function of the concentration of added Cu^{II}([13]aneS$_4$) for 45 (○), 55 (□), and 65 °C (▲). The value of $k_{11(ex)}$ at each temperature is obtained as the slope.

Table I. Self-Exchange Rate Constant Values for Cu$^{II/I}$([13]aneS$_4$) and Cu$^{II/I}$([15]aneS$_4$) As Determined from NMR Line-Broadening Measurements as a Function of Temperature in Deuterium Oxide Solution, Corrected to μ = 0.10 M (NO_3^-)

	$10^{-4}k_{11(ex)}$, M^{-1} s^{-1}		
		[15]aneS$_4$	
T, °C	[13]aneS$_4$	series I	series II
	Rate Constants		
5		0.63(8)	0.63(1)
15		0.90(2)	0.93(1)
25	32[a]	1.20(7)	1.23(5)
35		1.71(9)	1.87(7)
45	44(3)	2.05(5)	2.39(4)
55	53(3)		
65	58(3)		
	Activation Parameters		
ΔH^*, kJ mol^{-1}	10(1)	20(1)	22(1)
ΔS^*, J K^{-1} mol^{-1}	−106(7)	−101(5)	−92(5)

[a] Value of $k_{11(ex)}$ for Cu$^{II/I}$([13]aneS$_4$) at 25 °C is calculated from the experimentally determined activation parameters.

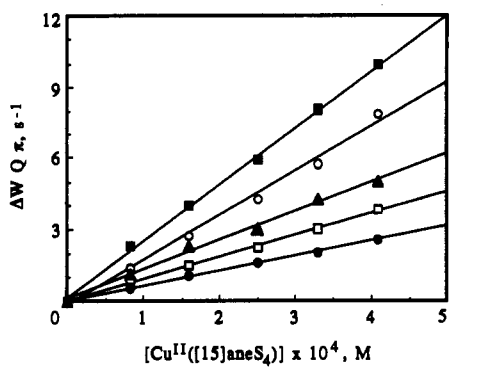

Figure 5. Plot of eq 3 for the NMR line-width data (series II) for Cu^I([15]aneS$_4$) as a function of the concentration of added Cu^{II}([15]aneS$_4$) for 5 (●), 15 (□), 25 (▲), 35 (○) and 45 °C (■). The value of $k_{11(ex)}$ at each temperature is obtained as the slope.

Kinetic Treatment for Rapid Second-Order Reactions. All cross reactions included in this study were of the general type represented in reaction 1 and were shown to exhibit second-order kinetic behavior in both directions as described by the following general expression:

$$\frac{dX}{dt} = k_{12}[A][B] - k_{21}[C][D] \quad (4)$$

where X represents the *increase* in product concentration subsequent to the time chosen as the "initial" time, and [A], [B], [C], and [D] represent the molar concentrations of $Cu^{II}L$, A_{Red}, $Cu^{I}L$, and A_{Ox}, respectively (see eq 1). (Cross reactions run in the reverse direction require a change in sign for the terms on the right side of eq 4.)

Most of the cross reactions involving $Cu^{II}L$ reduction were either extremely rapid or were limited in terms of the sensitivity of detection when operating under pseudo-first-order conditions. As a result, these reactions were run under second-order conditions. In analyzing the data, we have utilized a generalized second-order mathematical treatment which is applicable for reversible reactions where the second-order back-reaction may also contribute to the observed kinetics. Due to the configuration of the stopped-flow cell, a significant concentration gradient may also exist within the monitoring light path for very fast reactions immediately after mixing. The mathematical approach to this latter problem which we proposed earlier,[17] in which the reaction cell can be treated as a series of discrete segments, each containing different concentrations, was deemed unacceptable for reactions with free energies which are insufficient to drive the reactions to completion. Therefore, an alternative approach was taken in which the "initial" reaction time ($t = 0$) was selected at some arbitrary time after mixing. Under these conditions, some product formation will have already occurred for which a correction must be made for reversible reaction systems.[18]

The integration of eq 4 under conditions where the reverse reaction is appreciable and initial concentrations of the products may exist at the time selected as $t = 0$ has been presented previously.[8,19] The integrated expression can be rearranged to the following form:[8]

$$\frac{[C]_e[D]_e}{\sqrt{b^2 - 4ac}}\left\{\ln\left(\frac{2aX_t + b - \sqrt{b^2 - 4ac}}{2aX_t + b + \sqrt{b^2 - 4ac}}\right) - \ln\left(\frac{2aX_0 + b - \sqrt{b^2 - 4ac}}{2aX_0 + b + \sqrt{b^2 - 4ac}}\right)\right\} = k_{12}t \quad (5)$$

In eq 5, X_t represents the change in molar concentration of each of the reactants and products at any time, t, relative to their values at the selected zero time and the combined constant terms are defined as follows:

$$a = [C]_e[D]_e - [A]_e[B]_e$$

$$b = -\{([A]_0 + [B]_0)[C]_e[D]_e + ([C]_0 + [D]_0)[A]_e[B]_e\}$$

$$c = [A]_0[B]_0[C]_e[D]_e - [A]_e[B]_e[C]_0[D]_0$$

In these latter expressions, the subscripts e and 0 are used to designate the respective concentrations at equilibrium and at the selected zero time, respectively.

Cross Reactions Studied. For each copper system studied, several different oxidizing and reducing reagents were chosen for the cross-reaction studies as previously noted. The criteria for selecting the specific reagents utilized in these studies have been previously described.[8] Their pertinent physical properties are listed in Table II.

In the utilization of the second-order mathematical approach outlined above, the initial concentrations of the two reactant species were generally kept to within a ratio of 4:1 to 1:4. For the study of $Cu^{II}([13]aneS_4)$ reacting with $Ru^{II}(NH_3)_4bpy$, where the resolved second-order rate constants varied widely, comparative kinetic studies were also carried out under pseudo-first-order conditions in which the concentration of each reagent, in turn, was maintained in large excess (up to 12- or 50-fold).

The majority of the cross reactions involving $Cu^{I}L$ oxidation exhibited second-order rate constants below 10^7 M^{-1} s^{-1}, and many of these reactions were studied under pseudo-first-order conditions (which are not susceptible to error from concentration inhomogeneities). For the studies involving $Ni^{III}([14]aneN_4)$ as oxidizing agent, a wide range of oxidant concentrations was included in an attempt to identify the onset of limiting first-order kinetics representative of "gated" electron transfer.

For all reactions, seven or more replicate runs were generally carried out for each set of concentration conditions with a total of four to eight different concentration levels used in most studies. The rate constant values for each of the individual runs (over 600 total) and the mean values of the resolved second-order rate constants for each series of kinetic runs (i.e., with differing reactant concentrations) are compiled in the supplementary material. The overall rate constant values, as determined for each system, are summarized in Table III including the evaluated standard deviations.

Table II. Physical Properties of Reagents Used in This Work for Electron-Transfer Kinetic Studies with $Cu^{II/I}([13]aneS_4)$ and $Cu^{II/I}([15]aneS_4)$ in Aqueous Solutions at 25 °C, $\mu = 0.10$ M (ClO_4^-)

reagent	E^f, V	k_{22}, M^{-1} s^{-1}	$10^8 r$, cm[a]	log K_{12} (or K_{21}) Cu([13])	Cu([15])
Copper Complexes					
$Cu([13]aneS_4)^{2+/+}$	0.56[b]		4.4[d]	0.00	
$Cu([15]aneS_4)^{2+/+}$	0.64[c]		4.4[d]		0.0
Reductants					
$Co(Me_4[14]tetraeneN_4)^{2+}$	0.562[e]	5.0×10^{-3}[f]	4.7[d]	−0.03	1.32
$Ru(NH_3)_4bpy^{2+}$	0.526[g]	2.2×10^6[h]	4.4[d]	0.57	1.93
$Ru(NH_3)_5py^{2+}$	0.32[g]	1.1×10^5[h]	3.8[h]	4.06	5.41
$Ru(NH_3)_6^{2+}$	0.051[i]	4.3×10^3[h]	3.3[h]	8.60	9.96
Oxidants					
$Cu(Me_4[14]tetraeneN_4)^{3+}$	0.562[e]	5.0×10^{-3}[f]	4.7[d]	0.03	−1.32
$Ru(NH_3)_4bpy^{3+}$	0.526[g]	2.2×10^6[h]	4.4[d]	−0.57	−1.93
$Ni([14]aneN_4)^{3+}$	0.95[j]	1.0×10^3[j]	3.6[j]	6.59	5.24
$Ru(NH_3)_2(bpy)_2^{3+}$	0.889[k]	8.4×10^7[h]	5.6[h]	5.56	4.20
$Fe(4,7\text{-}Me_2phen)_3^{3+}$	0.939[d]	3.3×10^8[l]	6.6[d]	6.41	5.05

[a] Effective radius in forming the outer-sphere complex preceding electron transfer.[3] [b] Value shown is estimated from value determined in 80% methanol (see text). [c] Reference 22. [d] Reference 3. [e] Yee, E. L.; Cave, R. J.; Guyer, K. L.; Tyma, P. D.; Weaver, M. J. *J. Am. Chem. Soc.* **1979**, *101*, 1131–1137. Cf.: Endicott, J. F.; Durham, B.; Glick, M. D.; Anderson, T. J.; Kuszaj, J. M.; Schmonsees, W. G.; Balakrishnan, K. P. *J. Am. Chem. Soc.* **1981**, *103*, 1431–1440. [f] Corrected to $\mu = 0.10$ M from value determined in 1.0 M $HClO_4$: Durham, B. Ph.D. Dissertation, Wayne State University, 1977. [g] Yee, E. L.; Weaver, M. J. *Inorg. Chem.* **1980**, *19*, 1077–1079. [h] Brown, G. M.; Sutin, N. *J. Am. Chem. Soc.* **1979**, *101*, 883–892. [i] For 0.1 M $NaBF_4$: Lim, H. S.; Barclay, D. J.; Anson, F. C. *Inorg. Chem.* **1972**, *11*, 1460–1466. [j] Haines, R. I.; McAuley, A. *Coord. Chem. Rev.* **1981**, *39*, 77–119.. McAuley, A.; Macartney, D. H.; Oswald, T. *J. Chem. Soc., Chem. Commun.* **1982**, 274–275. Fairbank, M. G.; Norman, P. R.; McAuley, A. *Inorg. Chem.* **1985**, *24*, 2639–2644. [k] Seddon, E. A.; Seddon, K. R. *The Chemistry of Ruthenium*; Elsevier: New York, 1984; p 444. [l] Ruff, I.; Zimonyi, M. *Electrochim. Acta* **1973**, *18*, 515–516.

Discussion

Calculation of $k_{11(Red)}$ and $k_{11(Ox)}$ Values from Cross-Reaction Rate Constants. On the basis of the parameters listed for each of the counter reagents in Table II and the experimental cross-reaction rate constants in Table III, the apparent self-exchange rate constant values can be calculated for each $Cu^{II/I}L$ redox

(17) Lin, C. T.; Rorabacher, D. B. *J. Phys. Chem.* **1974**, *78*, 305–308.

(18) In the preparation of reducing reagents, it was sometimes observed that the reagents were not completely reduced or else were partially oxidized by exposure to air prior to initiating the mixing of the reactants. The mathematical approach described also makes allowance for the presence of product in the drive syringes.

(19) Smith, J. M. *Chemical Engineering Kinetics*, 2nd ed.; McGraw-Hill: New York, 1970; pp 60–65.

Table III. Summary of Electron-Transfer Cross-Reaction Rate Constants for $Cu^{II/I}([13]aneS_4)$ and $Cu^{II/I}([15]aneS_4)$ Reacting with Selected Oxidants and Reductants in Aqueous Solution at 25.0 °C, μ = 0.1 M ($HClO_4$), with All Data from This Work Except As Noted

	k_{12} or k_{21}, M^{-1} s^{-1} [a]	
reagent	$Cu^{II/I}([13]aneS_4)$	$Cu^{II/I}([15]aneS_4)$
reductants		
$Co^{II}Z(H_2O)_2$[b]	50[c]	2.2×10^2 [c]
$Ru^{II}(NH_3)_4bpy$	$1.8(6) \times 10^7$	$1.2(4) \times 10^6$
$Ru^{II}(NH_3)_5py$	$2.8(6) \times 10^7$	$9(2) \times 10^6$
$Ru^{II}(NH_3)_6$	$1.3(2) \times 10^8$	$3.3(5) \times 10^7$
oxidants		
$Co^{III}Z(H_2O)_2$[b]	55(7)[d]	1.36(8)
$Ru^{III}(NH_3)_4bpy$	$2.6(3) \times 10^5$	$7.8(7) \times 10^3$
$Ni^{III}([14]aneN_4)$	$4.92(3) \times 10^6$	$1.14(1) \times 10^5$
$Ru^{III}(NH_3)_2(bpy)_2$	$2.3(8) \times 10^7$	$8.4(1) \times 10^6$
$Fe^{III}(4,7\text{-}Me_2phen)_3$	$>1 \times 10^8$ [e]	$4.5(7) \times 10^7$
	1.8×10^6 [c]	*1.5×10^7* [c]

[a] In general, each rate constant value shown represents the median obtained from 3–8 different reagent concentrations with 7–8 repetitive runs for each set of conditions; numbers shown in parentheses represent standard deviations as calculated from the variation in mean values (for repetitive runs) and refer to the last digit shown {e.g., $4.93(3) \times 10^6$ represents $(4.92 \pm 0.03) \times 10^6$}. [b] The ligand abbreviated as Z represents $Me_4[14]tetraeneN_4$ (see text). [c] Data from ref 3. [d] Based on a very limited data set involving two runs at slightly different concentrations. [e] Limiting value based on observance of rates outside the range of the stopped-flow instrument.

couple from the cross-reaction kinetic data as previously described[3,8] using the Marcus relationship:[4]

$$k_{11(Red)} = (k_{12})^2 / \{k_{22} K_{12} f_{12} (W_{12})^2\} \quad (6a)$$

$$k_{11(Ox)} = (k_{21})^2 / \{k_{22} K_{21} f_{21} (W_{21})^2\} \quad (6b)$$

where k_{22} is the self-exchange rate constant of the counter reagent, $K_{12} = (K_{21})^{-1}$ is the equilibrium constant for reaction 1, f_{12} and f_{21} are nonlinear correction terms, and W_{12} and W_{21} are electrostatic work terms involved in bringing the reactants into outer-sphere contact.[3,8,20]

In calculating the K_{12} and K_{21} values en route to the k_{11} calculations, we have utilized a formal potential value of 0.56 V (vs NHE) for the $Cu^{II/I}([13]aneS_4)$ redox couple (Table II) rather than either of the previously reported values of 0.595 [21] or 0.52 V.[22] This adjustment was based on the observation that, whereas the potential for this couple has been difficult to establish accurately in aqueous solution, due to the tendency of the $Cu^{I}L$ species to precipitate on the electrode surface, the value obtained in 80% methanol–20% water (by weight), $E^f = 0.67$ V,[23] is believed to be much more accurate; and, as a general trend, the E^f values of the Cu(II/I) systems with the macrocyclic tetrathiaethers in aqueous solution tend to be approximately 0.10–0.11 V smaller than the 80% methanol values.[22]

The resulting calculated $k_{11(Red)}$ or $k_{11(Ox)}$ values from all cross-reaction studies are given in Table IV for both the $Cu^{II/I}([13]aneS_4)$ and $Cu^{II/I}([15]aneS_4)$ couples along with the 25 °C $k_{11(ex)}$ values determined from NMR measurements. For purposes of comparison, the corresponding k_{11} values previously reported for $Cu^{II/I}([14]aneS_4)$[7] are also included in this latter table.

Table IV. Electron Self-Exchange Rate Constants for $Cu^{II/I}([13]aneS_4)$, $Cu^{II/I}([14]aneS_4)$, and $Cu^{II/I}([15]aneS_4)$ As CAlculated from Cross-Reaction Rate Constants with Selected Oxidants and Reductants in Aqueous Solution at 25.0 °C, μ = 0.1 M ($HClO_4$)

	log k_{11}, M^{-1} s^{-1}		
reagent	$Cu^{II/I}$ ([13]aneS$_4$)	$Cu^{II/I}$ ([14]aneS$_4$)	$Cu^{II/I}$ ([15]aneS$_4$)
	NMR Method		
	5.50	3.88[a]	4.08
reductants			
$Co^{II}Z(H_2O)_2$[b]	5.59[c]	3.42[c]	3.70[c]
$Ru^{II}(NH_3)_4bpy$	5.87	3.79[a]	3.70
$Ru^{II}(NH_3)_5isn$[b]		4.02[a]	
$Ru^{II}(NH_3)_5py$	5.98	3.89[a]	4.00
$Ru^{II}(NH_3)_6$	5.28		3.11
oxidants			
$Co^{III}Z(H_2O)_2$[b]	5.52		3.76
$Ru^{III}(NH_3)_4bpy$	4.87	2.58[a]	3.26
$Ni^{III}([14]aneN_4)$	4.33	–0.1 to >3.2[a,d]	2.00
$Ru^{III}(NH_3)_2(bpy)_2$	1.89	0.1[a]	2.08
$Fe^{III}(4,7\text{-}Me_2phen)_3$	>2	≈0[a]	2.34
	–1.71[c]	–0.38[c]	*1.15*[c]

[a] Data from ref 8. [b] The ligand abbreviated as Z represents $Me_4[14]tetraeneN_4$; isn represents isonicotinamide. [c] Data from ref 3. [d] Calculated value of $k_{11(Ox)}$ was dependent upon concentration of the Ni(III) reagent as a result of the onset of gated electron-transfer conditions.

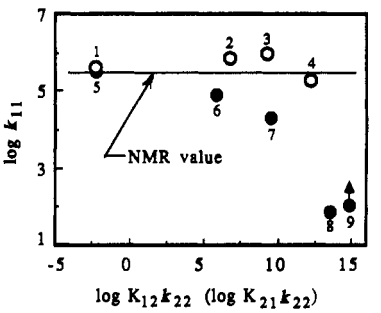

Figure 6. Plot of the logarithmetic values of the *apparent* self-exchange rate constants for $Cu^{II/I}([13]aneS_4)$, as calculated from the various cross reaction rate constants using the Marcus relationship, as a function of the "potential barrier parameter", log $K_{12}k_{22}$ (or log $K_{21}k_{22}$). The open circles represent reactions involving $Cu^{II}L$ reduction, while the solid circles are calculated from reactions involving $Cu^{I}L$ oxidation. The numbered points correspond to reactions with the counter reagents in the order listed in the tables: (1) $Co^{II}(Me_4[14]tetraeneN_4)$, (2) $Ru^{II}(NH_3)_4bpy$, (3) $Ru^{II}(NH_3)_5py$, (4) $Ru^{II}(NH_3)_6$, (5) $Co^{III}(Me_4[14]tetraeneN_4)$,(6) $Ru^{III}(NH_3)_4bpy$, (7) $Ni^{III}([14]aneN_4)$, (8) $Ru^{III}(NH_3)_2(bpy)_2$, (9) $Fe^{III}(4,7\text{-}Me_2phen)_3$.

Comparison of $k_{11(ex)}$, $k_{11(Red)}$, and $k_{11(Ox)}$ Values. As indicated in Table IV for each of the three systems, the self-exchange rate constant values calculated from cross reactions involving the *reduction* of a specific $Cu^{II}L$ species ($k_{11(Red)}$) are all within the same order of magnitude as the corresponding $k_{11(ex)}$ value determined by NMR line-broadening. For those $Cu^{I}([13]aneS_4)$ and $Cu^{I}([15]aneS_4)$ *oxidation* cross reactions which are relatively slow (i.e., those involving $Ru^{III}(NH_3)_4bpy$ and $Co^{III}(Me_4[14]tetraeneN_4)$ as oxidants), the calculated $k_{11(Ox)}$ values also appear to be within experimental error of the corresponding $k_{11(ex)}$ and $k_{11(Red)}$ values. However, as the product of $K_{21}k_{22}$ (the so-called "potential barrier parameter" from eq 6b)[8] increases (see Table II), the calculated values of $k_{11(Ox)}$ exhibit a significant decrease as illustrated in Figures 6 and 7.

As we have noted in our earlier investigation,[8] the generation of calculated $k_{11(Ox)}$ values which are significantly smaller than the directly determined $k_{11(ex)}$ value (from NMR line-broadening) is indicative of the onset of rate-limiting conformational control and, ultimately, of a change in the mechanistic pathway for the electron-transfer process. On the basis of the proposed mechanism

(20) In response to a reviewer's query regarding the possible influence of steric effects, it should be noted that the electrostatic work term includes corrections for both the charge and size of the reactants.

(21) Rorabacher, D. B.; Martin, M. J.; Koenigbauer, M. J.; Malik, M.; Schroeder, R. R.; Endicott, J. F.; Ochrymowycz, L. A. In *Copper Coordination Chemistry: Biochemical and Inorganic Perspectives*; Karlin, K. D., Zubieta, J., Eds.; Adenine: Guilderland, NY, 1983; pp 167–202.

(22) Bernardo, M. M.; Schroeder, R. R.; Rorabacher, D. B. *Inorg. Chem.* **1991**, *30*, 1241–1247.

(23) Dockal, E. R.; Jones, T. E.; Sokol, W. F.; Engerer, R. J.; Rorabacher, D. B.; Ochrymowycz, L. A. *J. Am. Chem. Soc.* **1976**, *98*, 4322–4324.

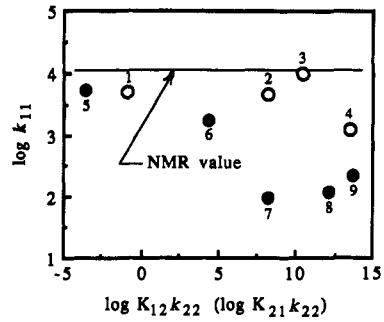

Figure 7. Plot of the logarithmetic values of the *apparent* self-exchange rate constants for $Cu^{II/I}([15]aneS_4)$, as calculated from the various cross reaction rate constants using the Marcus relationship, as a function of the "potential barrier parameter", log $K_{12}k_{22}$ (or log $K_{21}k_{22}$). The open circles represent reactions involving $Cu^{II}L$ reduction, while the solid circles are calculated from reactions involving $Cu^{I}L$ oxidation. The numbered points correspond to reactions with the counter reagents in the order listed in the tables and as identified in the caption to Figure 6.

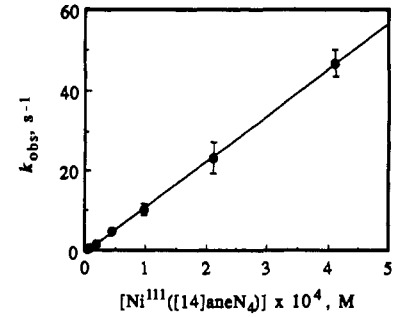

Figure 8. Plot of the observed pseudo-first-order rate constants for $Cu^{I}([15]aneS_4)$ reacting with $Ni^{III}([14]aneN_4)$ as a function of the concentration of the latter reagent. The error bars shown represent one standard deviation. The slope yields $k_{21} = (1.14 \pm 0.01) \times 10^5\ M^{-1}\ s^{-1}$. The excellent linearity of the plot indicates that the reaction conforms to second-order behavior over the entire 100-fold concentration range studied.

in Scheme I, the conditions required for such behavior can be derived from the overall kinetic expression for the *oxidation* of $Cu^{I}L$ which is of the following form:

$$-\frac{d[Cu^{I}L]}{dt} = \left(\frac{k_{2A}k_{RP}}{k_{2A}[A_{Ox}] + k_{PR}} + \frac{k_{2B}k_{QO}}{k_{B2}[A_{Red}] + k_{QO}}\right)[R][A_{Ox}] \quad (7)$$

where the first parenthetical term represents the contribution of pathway A and the second represents the contribution of pathway B. Four limiting expressions may be derived:

Pathway A dominant: $\left(\frac{k_{2A}k_{RP}}{k_{2A}[A_{Ox}] + k_{PR}}\right) >> \left(\frac{k_{2B}k_{QO}}{k_{B2}[A_{Red}] + k_{QO}}\right)$

If $k_{2A}[A_{Ox}] << k_{PR}$: $-\frac{d[Cu^{I}L]}{dt} = K_{PR}^{-1}k_{2A}[R][A_{Ox}]$ (7a)

If $k_{2A}[A_{Ox}] >> k_{PR}$: $-\frac{d[Cu^{I}L]}{dt} = k_{RP}[R]$ (7b)

Pathway B dominant: $\left(\frac{k_{2A}k_{RP}}{k_{2A}[A_{Ox}] + k_{PR}}\right) << \left(\frac{k_{2B}k_{QO}}{k_{B2}[A_{Red}] + k_{QO}}\right)$

If $k_{B2}[A_{Red}] << k_{QO}$: $-\frac{d[Cu^{I}L]}{dt} = k_{2B}[R][A_{Ox}]$ (7c)

If $k_{B2}[A_R] >> k_{QO}$: $-\frac{d[Cu^{I}L]}{dt} = K_{B2}^{-1}k_{QO}\frac{[R][A_{Ox}]}{[A_{Red}]}$ (7d)

In these expressions, $K_{PR}^{-1} = k_{RP}/k_{PR}$ and $K_{B2}^{-1} = k_{2B}/k_{B2}$. Theoretical considerations indicate that eq 7d will never apply to reactions which are thermodynamically favorable.[6] Thus, we may limit our current discussion to the first three expressions.

For the $Cu^{II/I}([14]aneS_4)$ system, ancillary low-temperature[7a] and rapid-scan[7b] electrochemical studies have established the fact that intermediate P is more stable than intermediate Q and, therefore, pathway A is intrinsically preferred. The observed trends in the calculated k_{11} values indicate that the same pathway preference applies to both the [13]- and [15]$aneS_4$ systems. Thus, if the rate of the cross reaction is sufficiently slow (i.e., $k_{2A}[A_{Ox}] \ll k_{PR}$), the species P and R will be equilibrated at all times, and eq 7a will apply. Under these circumstances, the calculated $k_{11(Ox)}$ value should be consistent with the $k_{11(ex)}$ value obtained from the NMR measurements—as is observed for the oxidation reactions involving $Ru^{III}(NH_3)_4bpy$ and $Co^{III}(Me_4[14]tetraeneN_4)$ as the counter oxidizing agents in the current study. Thus, the $k_{11(ex)}$, $k_{11(Red)}$, and the larger $k_{11(Ox)}$ values are representative of the self-exchange rate constant for $Cu^{II/I}L$ proceeding by pathway A (i.e., $k_{11(A)}$).

As the product $K_{21}k_{22}$ increases, k_{2A} also increases until $k_{2A}[A_{Ox}]$ exceeds the value of k_{PR} and the rate of conformational change R → P becomes the rate-determining step (eq 7b), representing the condition known as "gated" electron transfer. In our previous study on $Cu^{II/I}([14]aneS_4)$,[8] we were able to demonstrate the onset of gated behavior by varying the concentration of the $Ni^{III}([14]aneN_4)$ reagent over a 1000-fold range and noting that the cross reaction was first-order over much of this range. In the current investigation, similar studies on the $Cu^{I}([13]aneS_4)$ system resulted in cross reactions which were so rapid that the concentration of the Ni^{III} reagent was limited to a 5-fold range over which a seemingly consistent second-order rate constant value was obtained (see supplementary material). Although the apparent $k_{11(Ox)}$ value calculated from the $Ni^{III}([14]aneN_4)$ cross reaction is more than 1 order of magnitude smaller than the $k_{11(ex)}$ and $k_{11(Red)}$ values for this system, it is closer to these values (and almost within the limits of the presumed experimental error) than it is to the $k_{11(Ox)}$ value obtained for the corresponding $Cu^{I}([13]aneS_4)$ oxidation with $Ru^{III}(NH_3)_2(bpy)_2$, which we presume represents reaction via pathway B (eq 7c). Thus, we postulate that the $Cu^{I}([13]aneS_4)$ reaction with $Ni^{III}([14]aneN_4)$ is predominantly following pathway A under the conditions utilized, although some contribution from conformational "gating" may be tending to slow down the reaction in the accessible concentration range. This observation permits us to set a lower limit on k_{RP} of $\geq 200\ s^{-1}$ since, at the highest concentration level of $Ni^{III}([14]aneN_4)$ for which viable kinetic data were obtained, the mean reaction lifetime was approximately 4.7 ms (see supplementary material). Thus, the rate constant for conformational gating is at least four times larger than the corresponding value for $Cu^{II/I}([14]aneS_4)$ ($k_{RP} = 50\ s^{-1}$).

For the $Cu^{I}([15]aneS_4)$ system, the cross reactions with $Ni^{III}([14]aneN_4)$ were significantly slower permitting kinetic measurements to be made over a 100-fold range of reagent concentration. As illustrated in Figure 8, this reaction appears to exhibit consistent second-order behavior throughout this extended concentration range. Moreover, the apparent $k_{11(Ox)}$ value obtained by applying the Marcus relationship to the resolved k_{21} value for this cross reaction was about 2 orders of magnitude smaller than the corresponding $k_{11(ex)}$ and $k_{11(Red)}$ values and appears to be in agreement with the $k_{11(Ox)}$ values obtained for the cross reactions with $Ru^{III}(NH_3)_2(bpy)_2$ and $Fe^{III}(4,7\text{-}Me_2\text{-}phen)_3$. Therefore, it is likely that all three of the latter reactions represent pathway B. On the basis of the cumulative kinetic data (see supplementary material), we estimate that k_{RP} may be $\leq 5\ s^{-1}$. As an important consequence of the fact that the two alternate pathways are energetically closer together for the [15]$aneS_4$ system, the range of conditions over which gated behavior will be manifested is severely limited. This fact is largely responsible for our inability to access the gated region during this study.

The cumulative results suggest that, for all three Cu(II/I) systems represented in Table IV, the reactions involving $Ru^{III}(NH_3)_2(bpy)_2$ and $Fe^{III}(4,7\text{-}Me_2phen)_3$ as oxidizing reagents are representative of a switch to pathway B as the dominant mechanistic pathway such that the calculated $k_{11(Ox)}$ values are representative of $k_{11(B)}$. For the [15]aneS$_4$ system, this switch has also already occurred with the Ni(III) reagent whereas, for the [13]aneS$_4$ system, the kinetics for the Ni(III) reaction may just be entering the gated regime under the conditions accessible in our study. By contrast, the cross reaction between Cu^{I}([14]aneS$_4$) and Ni^{III}([14]aneN$_4$) is in the transition range in which the reaction is gated by the rate constant for conformational change, k_{RP}.

Conclusions. From the foregoing observations, we conclude that the results for the two systems involved in the current study are consistent with those previously found for the $Cu^{II/I}$([14]aneS$_4$) investigation with some interesting contrasts. Since the activation parameters are similar for the [14]aneS$_4$ and [15]aneS$_4$ systems ($\Delta H^{\ddagger}$ = 24 ± 1 [8] and 21 ± 1 kJ mol^{-1}, respectively; $\Delta S^{\ddagger}$ = −92 ± 3 [8] and −97 ± 7 J K^{-1} mol^{-1}, respectively) it is presumed that pathway A is energetically equivalent for both systems. However, for the $Cu^{II/I}$([15]aneS$_4$) system, the difference in the Cu(II/I) self-exchange rate constants representative of the two pathways (i.e., $k_{11(A)} \approx 1 \times 10^4$ M^{-1} s^{-1} and $k_{11(B)} \approx 1 \times 10^2$ M^{-1} s^{-1}) is much smaller making it apparent that pathway B has become more available for the latter system. This implies that intermediate Q is more stable (i.e., less unstable) in this latter case. Since we have previously surmised that the coordination geometry of species Q is similar to that of R,[8] this may be interpreted to indicate that the expanded ring in [15]aneS$_4$ can more easily undergo the distortions necessary to achieve a tetrahedral coordination sphere around the copper ion, a fact which is consistent with molecular models.

It is especially interesting to note that the $k_{11(ex)}$ value for $Cu^{II/I}$([13]aneS$_4$) is one of the largest self-exchange rate constants reported to date in aqueous solution for a low molecular weight Cu(II/I) system.[24] This value is slightly larger than—though comparable to—the corresponding values recently determined for two quinquedentate ligand systems, $Cu^{II/I}$([15]aneS$_5$) {$k_{11(ex)} = 2 \times 10^5$ M^{-1} s^{-1}}[14] and the analogous $Cu^{II/I}$([15]aneNS$_4$) {$k_{11(ex)} = 1.4 \times 10^5$ M^{-1} s^{-1}}.[15] Crystallographic structural determinations have shown that Cu^{II}([15]aneS$_5$) exhibits a square pyramidal geometry and that reduction to Cu^{I}([15]aneS$_5$) involves the rupture of a Cu–S bond to produce a distorted tetrahedral complex.[25] As shown in Figure 1C, Cu^{II}([13]aneS$_4$) has a similar structure to that of the Cu^{II}([15]aneS$_5$) complex except that a solvent molecule (or anion) occupies the apical position in the former species whereas the fifth sulfur donor atom occupies this site in Cu^{II}([15]aneS$_5$). Reduction to Cu^{I}([13]aneS$_4$) is also presumed to involve the rupture of a Cu–S bond (Figure 1D) so that the overall structural change upon reduction is apparently very similar for the [15]aneS$_5$ and [13]aneS$_4$ systems. The consistency of the $k_{11(ex)}$ activation parameters for these two systems ($\Delta H^{\ddagger}$ = 14 ± 4 [14] and 10 ± 1 kJ mol^{-1}, respectively; $\Delta S^{\ddagger}$ = −103 ± 11 [14] and −106 ± 7 J K^{-1} mol^{-1}, respectively) strongly suggests that the dominant reaction pathway is similar for the two systems and implies that Cu–S bond rupture does not impose a high energy barrier on the overall kinetics.

On the basis of the lower limit estimated for the rate constant representing conformational change in the oxidation of Cu^{I}([13]aneS$_4$) via pathway A ($k_{RP} \geq 200$ s^{-1}), this conformational change is rapid and gated behavior is, therefore, difficult to demonstrate using the stopped-flow technique. For Cu^{I}([15]aneS$_4$) oxidation via pathway A, conformational change is a much slower process but the reduced energy gap between the two pathways leads to a narrow band of conditions in which the gated region may be sampled directly, conditions which we were apparently unable to achieve with the reagents used in the current work. Thus, of the systems we have studied in depth, only $Cu^{II/I}$([14]aneS$_4$) has provided us with a direct demonstration of the gated region.[8] Further studies are currently underway to broaden our understanding of the gated phenomenon itself and to establish the influence of specific structural parameters upon the magnitude of k_{RP}.

Acknowledgment. Part of this work was supported by a contract from the Getty Conservation Institute. The authors wish to acknowledge the Central Instrumentation Facility at Wayne State University for making available the NMR spectrometers used in this research as well as other ancillary equipment. The authors also express their appreciation to Professors Morton Raban and John P. Oliver for helpful discussions regarding the interpretation of the NMR spectra.

Supplementary Material Available: Tables listing original NMR linewidth data and original stopped-flow kinetic data (14 pages). Ordering information is given on any current masthead page.

(24) A comparable self-exchange rate constant, 5.5 × 10^5 M^{-1} s^{-1}, has been reported in methanolic solution for the porphyrin-like system (tetrabenzo[*b*,*f*,*j*,*n*][1,5,9,13]tetraazacyclohexadecine)copper(II/I): Pulliam, E. J.; McMillan, D. R. *Inorg. Chem.* **1984**, *23*, 1172–1175. In addition, Swaddle and co-workers have reported a self-exchange rate constant of 5.0 × 10^5 M^{-1} s^{-1} for bis(2,9-dimethyl-1,10-phenanthroline)-copper(II/I) in D_2O: Doine, H.; Yano, Y., Swaddle, T. W. *Inorg. Chem.* **1989**, *28*, 2319–2322.

(25) Corfield, P. W. R.; Ceccarelli, C.; Glick, M. D.; Moy, I. W.-Y.; Ochrymowycz, L. A.; Rorabacher, D. B. *J. Am. Chem. Soc.* **1985**, *107*, 2399–2404.